Optical Tweezers

Kyungmin Yu*
Department of Materials Science and Engineering,
Seoul National University
1, Gwanak-ro, Gwanak-gu, Seoul, Republic of Korea
E-mail: yukm0227@snu.ac.kr
(Dated: April 10, 2024)

Optical tweezers are apparatus to capture tiny specimens such as cells or micrometer-scale beads. In this experiment, the trapping force of the optical tweezers was measured based on the theory of Brownian motion and drag force. The drag coefficients for the specimen were obtained by Brownian motions and the obtained viscosity of water was reasonable compared to the value in the literature. It was assumed that the drag force was in equilibrium with the trapping force. The trapping force was linearly increased as the current of LASER increased. For the current of 70 mA, the trapping force was estimated to be about 0.3 - 1.5 pN. It must be noted that the trapping force was maximal for the sample with diameter 2.07 µm. This maximum seems to stem from the similarity between the size of the bead and the diameter of the LASER. Also, there was a threshold current that LASER started to emit the light. By the extrapolation of the linear trend line, the threshold current was estimated to be about 30 mA, which is lower than the value noted in the handbook of LASER (35 mA). The deviation of 3.0 µm sample was explained by the friction between beads and slide/cover glass. In addition, the configuration of the specific number of beads under the optical tweezers was investigated.

I. INTRODUCTION

Optical tweezers are an apparatus to make a tiny specimen stationary with a strongly focused light. According to the theory of optics, light exerts a force that is proportional to the gradient of intensity. The force exerted by a well-aligned optical apparatus enables the precise control of micrometer-scale specimens without damage. Therefore, optical tweezers can be applied not only in biological sciences but also in other fields. For instance, it is possible to measure the mechanical properties of red blood cells with optical tweezers. Besides, optical tweezers are in use for the assembly of micro-scale devices and machines. [1]

In the operation of optical tweezers, it is important to quantify the force exerted by the light. The goal of this experiment is to measure the trapping force of the optical tweezers with the silica colloidal solution specimen. In this case, the trapping force can be measured from the drag force exerted by solvent which is in equilibrium with the trapping force. The drag force can be attained from the Stokes law for drag force, then it is essential to get the drag coefficient. In this experiment, we measured the drag coefficient by the Brownian motion of a specimen particle. Thereby, it was possible to measure the drag force and the trapping force of optical tweezers.

A. Background: Optical Tweezers

Optical tweezers are based on the momentum exerted by the light. In the medium of refractive index n, the force F exerted by the light with power P is like (1).

$$F = \frac{nP}{c} \tag{1}$$

There are mainly two forces acting on the specimen: gradient force and scattering force. Gradient force points in the direction of the intensity gradient of the incident light, while scattering force points in the direction of the incident light. To generate an optical trap, the gradient force needs to exert a recovery force and its magnitude must surpass that of the scattering force. To exert a recovery force, the intensity of the LASER beam needs to be Gaussian. Therefore, TEM00 (Transverse Electromagnetic Mode) LASER, of which intensity distribution is nearly Gaussian is commonly used for optical tweezers. [1]

If the dimension of the specimen is much larger than the wavelength, it is possible to obtain the difference of the light momentum before and after passing through the specimen with a geometrical consideration. This condition is the so-called 'ray-optics regime'. A. Ashkin reported the optical trap for the spherical specimen in the ray-optics regime. [2] Out of the ray-optics regime, it is necessary to consider general gradient force and general scattering force. For a very small specimen, the scattering force may be calculated in the regime of Rayleigh scattering. In this case, the Gaussian-form gradient force needs to surpass the scattering force to generate the recovery force field.

* Also at Department of Physics and Astronomy, Seoul National University. (Double major)

B. Background: Brownian Motion

To measure the drag coefficient for the silica bead, Brownian motion can be applied. Brownian motion is a stochastic motion of microscopic particles in the fluid, due to the collision with the fluid particles and the given microscopic particles. The silica bead in water receives the external force by Brownian motion F_{ext} and the drag force proportional to the velocity, $-\mu v$. Equation of motion for the silica bead can be written like (2).

$$m\frac{d^2x}{dt^2} = -\mu\frac{dx}{dt} + F_{\text{ext}} \tag{2}$$

When the time average is applied on both sides, F_{ext} term will be zero given that the Brownian motion is a stochastic process. Then, equation (2) will be converted like (3) with some simple calculations, where g is defined like (4).

$$m\frac{dg}{dt} - \left\langle mv_x^2 \right\rangle + \mu g = 0 \tag{3}$$

$$g = \left\langle x\frac{dx}{dt} \right\rangle \tag{4}$$

By the equipartition theorem, (3) can be converted like (5).

$$m\frac{dg}{dt} + \mu g = \frac{1}{2}k_BT \tag{5}$$

Solving the differential equation for g with the initial condition $g(0) = 0$, the solution is like (6).

$$g(t) = \frac{1}{2}\frac{d\left\langle x^2 \right\rangle}{dt} = \frac{k_BT}{\mu}(1 - e^{-\frac{\mu}{m}t}) \tag{6}$$

In the condition of $t \gg m/\mu$, the expression for $\left\langle x^2 \right\rangle$ is derived like (7).

$$\left\langle x^2 \right\rangle \simeq \frac{2k_BT}{\mu}t \tag{7}$$

Given that the motion in the experiment is 2-dimensional, the expression for $\left\langle r^2 \right\rangle$ is like (8).

$$\left\langle r^2 \right\rangle \simeq \frac{4k_BT}{\mu}t \tag{8}$$

Also, since the specimen is sphere-shaped, it is possible to apply the Stokes formula of drag force, (9).

$$f = 6\pi\eta a v \tag{9}$$

Namely, the viscosity of the fluid can be expressed like (10).

$$\eta = \frac{\mu}{6\pi a} \tag{10}$$

The video analysis for the Brownian motion enables the calculation of the value of μ, then it is possible to get the viscosity of the fluid.

II. MATERIALS AND METHODS

A. Preparation of the Sample

Four kinds of spherical silica beads colloidal solutions were prepared. For each solution, one drop of silica beads colloidal solution (Polysciences, Inc.) was diluted in 15 mL of distilled water. The diameters of silica beads were 0.51 µm, 1.06 µm, 2.07 µm and 3.0 µm. About 20 µL of diluted solution was dropped on a slide glass, then a cover glass was put on the drop carefully not to make air bubbles inside the specimen.

B. Observation of the Sample

For the optical trapping and observation, Portable Optical Tweezers Educational Kit (Thorlabs, Inc.) was employed. After the LASER and the camera attached to the kit was turned on, the specimen was loaded on the stage of the device and the focus point was found. To avoid a collision between the lens and the specimen, the stage was placed as low as possible during the sample loading, then it ascended to find the focus point. During the focusing procedure, three focus points were found: (i) at the upper part of the cover glass, (ii) at the lower part of the cover glass, (iii) at the sample under the cover glass. When the focus point was fixed to the (iii), the stage was moved slightly to locate a bead directly under the LASER beam. As above, the focus point and the location of the bead were tuned, and then their trapping by the LASER was observed through the camera.

C. Measurement of the Viscosity

To measure the viscosity, the Brownian motion of the beads was recorded through the camera. After setting the focus point, the scale bar was set first. Observing the specimen, some stationary beads did not show any Brownian motions. Based on these beads, the scale bar in the video was constructed. The stage was translated by such distance, and the initial and the final locations of the stationary bead were marked. After that, the motions of the beads were recorded. The motion of certain beads was analyzed by Tracker, which is an open-source program to track the trajectory of certain points. According to (8), the expectation value of r^2 during the Brownian motion is proportional to time. Therefore, at least five motions of beads were tracked for each specimen and the value of r^2 was averaged. Then, the linear trend line and its gradient were obtained. Since (8) implies that this value is approximately $4k_BT/\mu$, the temperature of the laboratory was measured and the value of μ was derived. With (10), the viscosity could be obtained.

D. Measurement of the Trapping Force

With the value of viscosity obtained in the previous subsection, the drag force can be calculated based on (9). The trapping force of the optical tweezers can be measured by moving the bead with the optical tweezers at different speeds. For instance, if the bead started not to be dragged with a certain speed, that implies the threshold of equilibrium. Namely, the trapping force of the optical tweezers is equal to the drag force at the moment. In this method, it is possible to measure the trapping force of the optical tweezers. In addition, the trapping force can be obtained for different current values of the LASER. The change of the optical tweezers' trapping force by the LASER current was analyzed. Also, by extrapolating the tendency between the trapping force and the LASER current, the threshold current of the LASER could be estimated.

E. Additional Experiments

Some additional experiments aside from the given manual were conducted. The mainly analyzed topic was trapping multiple beads at once. Trapping one bead, the LASER can be moved to trap another bead. In this way, it is possible to trap multiple beads at once. For the specific number of trapped beads, the configuration of them under the LASER was determined. After trapping multiple beads, the LASER was slightly moved with an appropriate speed to make the configuration reach a stable equilibrium. Then, the possible configurations were observed through the camera and noted for each number of beads.

III. RESULT

A. Measurement of the Viscosity

The Brownian motions were observed and analyzed for three samples with diameters 1.06 µm, 2.07 µm and 3.0 µm. The five trajectories of Brownian motions for each sample are shown in FIG. 1a to FIG. 1c with five different colors. From the trajectories, the r^2 values according to time for each trajectory were calculated and plotted in FIG. 2a to FIG. 2c. Five curves of which color is the lightest show five $r^2 - t$ graphs of each trajectory. Then, for each time, five r^2 values were averaged and plotted as a black bold curve. Black dotted lines imply the 1σ range for the five trajectories. Given that $\langle r^2 \rangle$ and t is linear according to the equation (8), Linear regression for the $\langle r^2 \rangle - t$ curve was conducted and showed as a red solid line. Red dotted lines imply the 1σ range for the linear regression. For the linear regression, R^2 value and the equation of the trend line including the error are given in the figures.

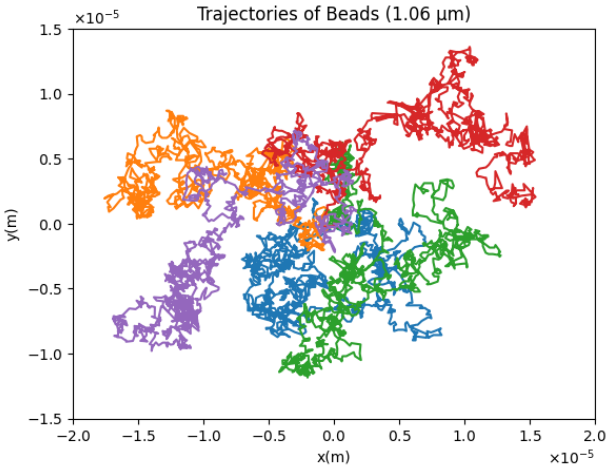

FIG. 1a. Trajectories of beads with diameter 1.06 µm.

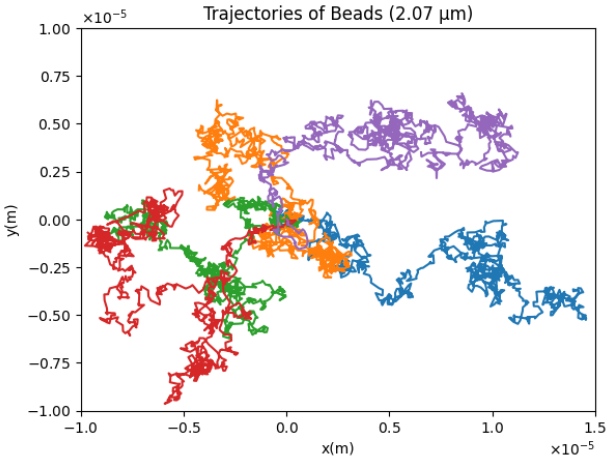

FIG. 1b. Trajectories of beads with diameter 2.07 µm.

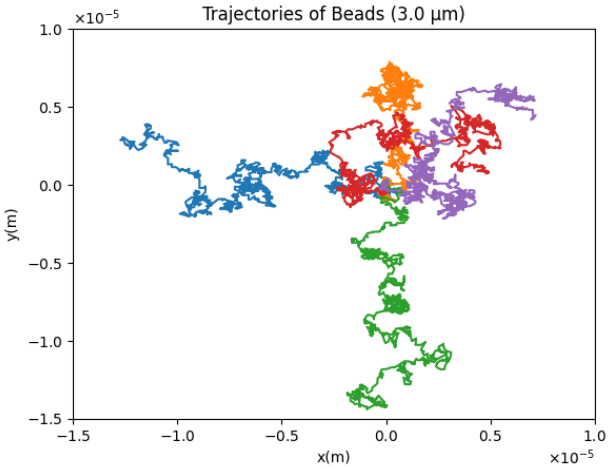

FIG. 1c. Trajectories of beads with diameter 3.0 µm.

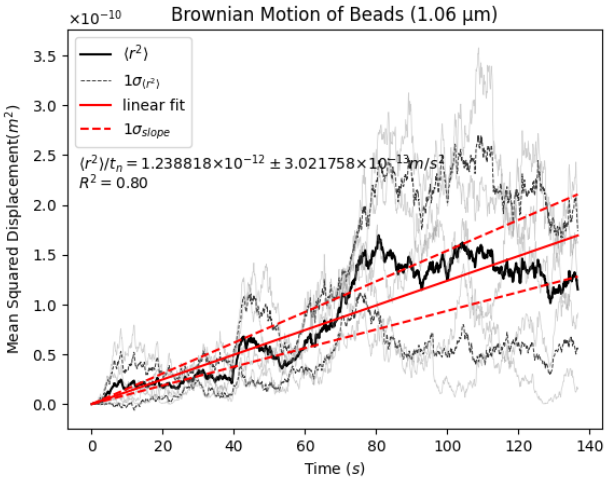

FIG. 2a. $r^2 - t$ graph for beads with diameter 1.06 μm.

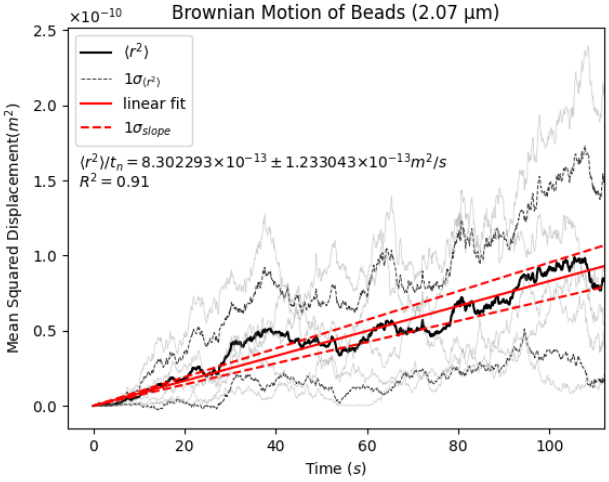

FIG. 2b. $r^2 - t$ graph for beads with diameter 2.07 μm.

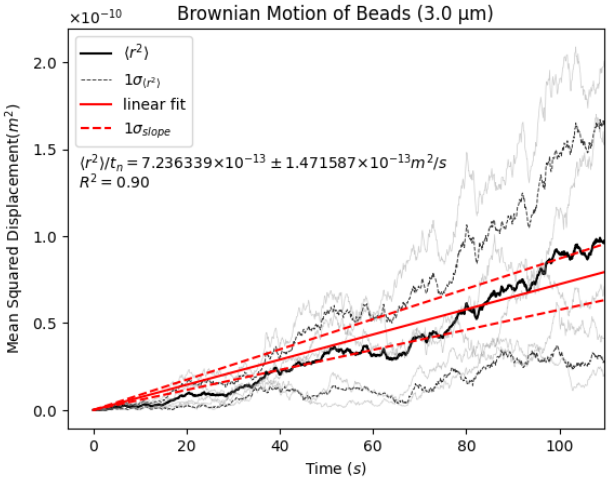

FIG. 2c. $r^2 - t$ graph for beads with diameter 3.0 μm.

According to the equation (8), the slope of $\langle r^2 \rangle - t$ trend line is equal to $4k_BT/\mu$. Note that the temperature of the laboratory was measured to be 294.95 K. Also, the drag coefficient has a relation with the viscosity as the equation (10). Therefore, the viscosity of water can be derived as the equation (11).

$$\eta = \frac{4k_BT}{6\pi a} \times \frac{1}{(\text{slope})} \tag{11}$$

Based on (11), the viscosity of water can be calculated and the result is shown in TABLE I. Given that the viscosity of water is 1.0016 mPa [3], the calculated viscosity is pretty reasonable.

TABLE I. Viscosity of water derived from the Brownian motions of each sample.

sample	slope [m^2/s]	viscosity [mPa · s]
1.06 μm	$(1.239 \pm 0.302) \times 10^{-12}$	1.316 ± 0.321
2.07 μm	$(8.302 \pm 1.233) \times 10^{-13}$	1.006 ± 0.149
3.0 μm	$(7.236 \pm 1.472) \times 10^{-13}$	0.796 ± 0.162

B. Measurement of the Trapping Force

The apparatus that was used in this experiment can move the stage with a set velocity. To measure the trapping force, the velocity of the stage was tuned to find the threshold that a bead gets lost during the movement. The threshold velocity implies the point that the Stokes' drag force surpasses the trapping force of the optical tweezers. The threshold velocity was found manually, and repeated by three times to get the standard deviation errors. Also, this test was conducted for various values of current for LASER. For four samples with diameters 0.51 μm, 1.06 μm, 2.07 μm and 3.0 μm, the relation between the threshold velocity and the LASER current was shown in FIG. 3a to FIG. 3d. Data points and 1σ error bars are shown as black dots and bars. Then, linear regression was conducted given that the data seemed to show linear relationships. The R^2 values for each linear regression are given, which show strong linear relationships. For the linear regressions, 1σ errors are shown as light red regions.

Given that the trapping force and the Stokes' drag force are in equilibrium, the trapping force can be expressed as (12), where v_{th} terms the threshold velocity.

$$F_{\text{trap}} = 6\pi a \eta v_{\text{th}} \tag{12}$$

Based on (12), the trapping force for each sample when the LASER current is 70 mA is given in TABLE II. It must be noted that the value of viscosity was obtained from TABLE I. Since the viscosity of water for the 0.51 μm sample was not measured, the viscosity value of water for the 0.51 μm sample was obtained from the reference [3]. Note that the error values of viscosity and threshold velocity were omitted in TABLE II.

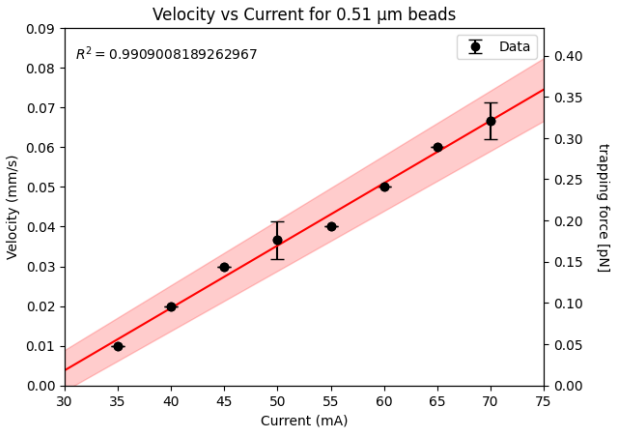

FIG. 3a. Threshold velocity - LASER current relationship of the sample with diameter 0.51 µm.

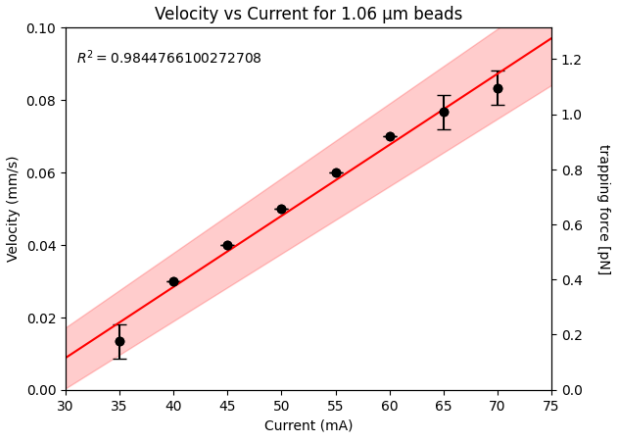

FIG. 3b. Threshold velocity - LASER current relationship of the sample with diameter 1.06 µm.

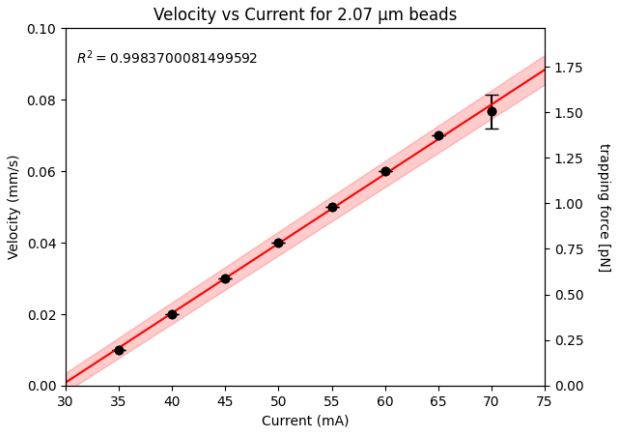

FIG. 3c. Threshold velocity - LASER current relationship of the sample with diameter 2.07 µm.

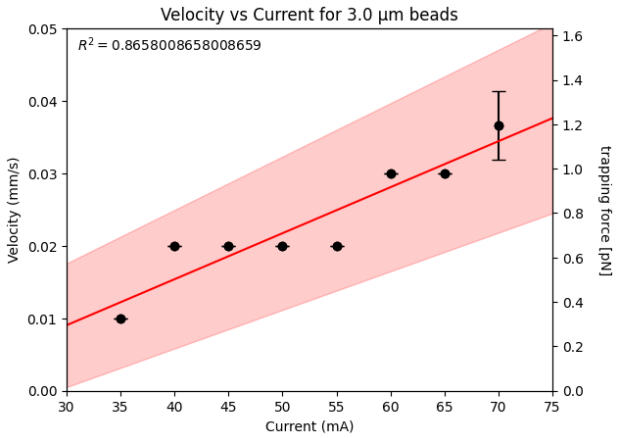

FIG. 3d. Threshold velocity - LASER current relationship of the sample with diameter 3.0 µm.

TABLE II. Trapping force of each sample when the LASER current is 70 mA.

sample	viscosity [mPa·s]	v_{th} [mm/s]	trapping force [pN]
0.51 µm	1.002	0.0667	0.321 ± 0.0235
1.06 µm	1.316	0.0833	1.096 ± 0.0489
2.07 µm	1.006	0.0767	1.505 ± 0.0956
3.0 µm	1.154	0.0367	1.196 ± 0.138

TABLE III. Threshold current of the LASER obtained from each sample.

sample	threshold current [mA]
0.51 µm	27.6 ± 2.36
1.06 µm	25.5 ± 3.05
2.07 µm	29.6 ± 1.01
3.0 µm	15.7 ± 9.00

It must be noted that the trapping force was maximal when the diameter of the sample was 2.07 µm. This maximum may stem from the similarity between the size of the LASER beam and the dimension of the bead. The detailed discussion will be conducted in the subsection IV B.

The threshold current to make the LASER emit light can be estimated from the x-intercept of the linear trend line. The estimated values are in TABLE III. Note that the threshold current of the LASER in the handbook was 35 mA. The calculated threshold current was slightly lower than the value in the handbook within the reasonable range. It must be highlighted that the obtained threshold current is deviated for the sample with diameter 3.0 µm. The linearity of data points for 3.0 µm are much lower than the other samples, referring to the lower R^2 value of the linear trend line. The substantiation of this phenomenon will be described in the subsection IV B.

C. Configuration of Beads in Multiple Trapping

The configuration of beads when multiple beads were simultaneously trapped by the optical tweezers is shown

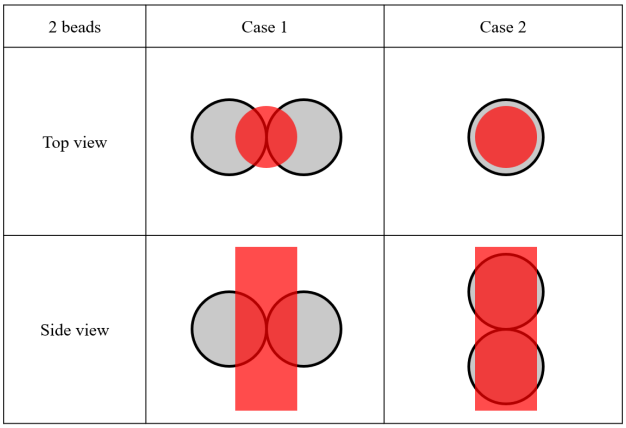

FIG. 4a. Two stable configurations for two beads trapping.

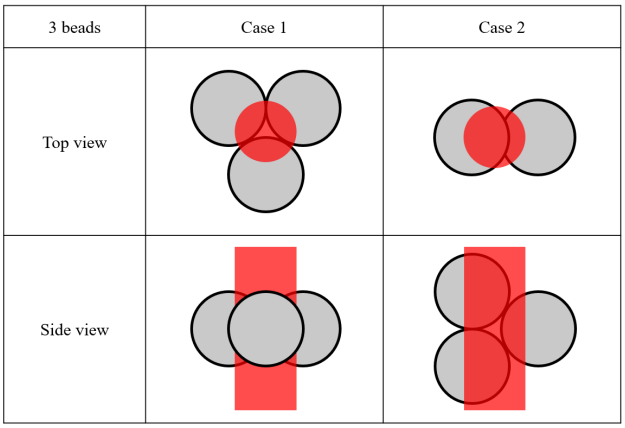

FIG. 4b. Two stable configurations for three beads trapping.

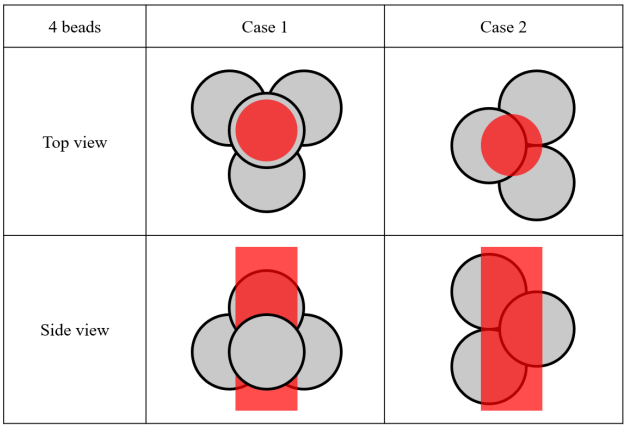

FIG. 4c. Two stable configurations for four beads trapping.

in FIG. 4a to FIG. 4c. Dark circles with black boundaries denote the beads. Red shapes denote the LASER beam, where the circle is the top view of the LASER beam and the rectangle is the side view of the LASER beam. For two beads, the stable configurations of beads are all linear. For case 1, the direction of alignment is perpendicular to the LASER beam direction, while it is parallel to the LASER beam direction in case 2. For three beads, the stable configurations of beads are triangular. The triangular shape has different alignments like FIG. 4b. For four beads, the stable configurations of beads are tetrahedral, where cases 1 and 2 show two different orientations of the tetrahedron. Note that the configurations are all identical for a certain number of beads except for their orientation.

IV. DISCUSSION

A. Measurement of the Viscosity

1. *Verification of Randomness in the Brownian Motion*

To measure the viscosity of water and the drag coefficient, it was assumed that beads are under Brownian motion due to the stochastic motion of water molecules. Referring to the equation 2, the external force acting on beads by water molecules was assumed to be perfectly random to average out F_{ext} term. To verify the randomness of the motion of beads, the Quantile-Quantile plot (Q-Q plot) was plotted. Q-Q plot can qualitatively check whether two distributions are identical or not. Two distributions are sorted in ascending order and placed on each axis. The more similar the two distributions are, the more linear the Q-Q plot is. Given that the motion of a bead was assumed to be Brownian, the velocity distribution of a bead must be Gaussian. Therefore, the Q-Q plot comparing the Gaussian distribution and the actual velocity distribution of a bead is shown in FIG. 5a to FIG. 5c. Note that the velocity was obtained from the finite difference of position. If the one-step finite difference of position is applied, there is too much fluctuation. To eliminate such fluctuation, the average of $n-1$th, nth, and $n+1$th finite difference was applied as a velocity value for nth step.

From the Q-Q plot with a linear shape, it is possible to claim that the beads are under the Brownian motions. However, there is a little deviation from the Gaussian distribution as shown at the right end of the Q-Q plot which directs upward. This deviation seems to stem from the net flow of water in a certain direction. However, the net flow effect was not considered in this experiment. There are some air bubbles inside the sample which are not able to be eliminated due to technical limitations. When these bubbles burst, the direction and magnitude of the net flow change, and it is impossible to calculate the accurate net flow due to this alteration. It was confirmed that if the net flow effect was considered, the linear trend line of $\langle r^2 \rangle - t$ curve shows a much lower R^2 value compared to that without the net flow effect. Therefore, the new flow effect was not considered, and the Q-Q plot shows a little deviation.

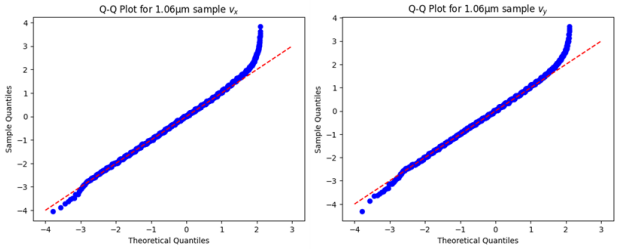

FIG. 5a. Q-Q plot for v_x and v_y of 1.06 µm sample.

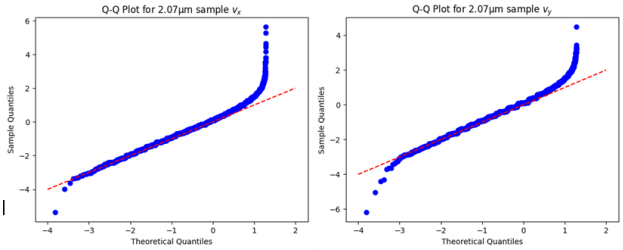

FIG. 5b. Q-Q plot for v_x and v_y of 2.07 µm sample.

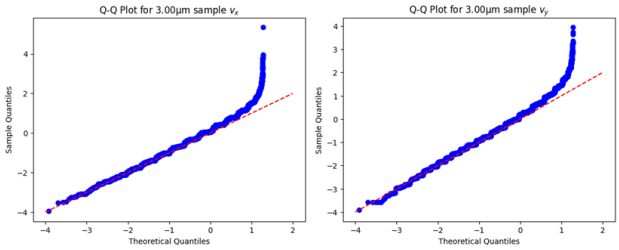

FIG. 5c. Q-Q plot for v_x and v_y of 3.0 µm sample.

2. *Non-ideal Factors in the Stokes' Formula*

In TABLE I, it was verified that the obtained viscosity is reasonable considering the viscosity of water in the literature. The error was about 30 % and its cause must be discussed further. The viscosity was calculated from the Stokes' drag force formula like the equation (9). However, this equation is valid for the laminar flow of the fluid. If there are any turbulence or obstacles in the fluid, Stokes' formula will deviate from the ideal circumstance. Since the sample contains many beads, the target bead may interact with other beads. Movements of other beads may generate turbulence, which makes Stokes' formula fail to predict the drag force. Therefore, the error is inevitable since it is almost impossible to consider every non-ideal factor such as turbulence or interactions of beads. To sum up, as long as Stokes' formula is employed to calculate the drag force, the error due to the non-ideal behavior of the fluid and beads must occur.

B. Measurement of the Trapping Force

1. *Magnitude of Trapping Forces*

It was highlighted that the trapping force is maximal for the 2.07 µm sample. This maximum seems to originate from the fact that the size of the LASER beam is similar to the size of the bead. If the bead is much smaller than the LASER beam, the circumferential part of LASER does not exert any light pressure on the bead. On the contrary, if the bead is much larger than the LASER beam, the light will not change its direction due to the large radius of curvature. In the ray-optics regime, the direction change of light determines the exerted momentum on the bead. Although the size of the bead is not proper to apply the ray-optics regime, a similar effect is anticipated. Therefore, if the dimensions of the LASER beam and the bead match well, the trapping force may be maximized. The quantitative condition to maximize the trapping force is complicated since it is impossible to apply the ray-optics regime in this experiment. In addition, the 3.0 µm sample is noteworthy in terms of smaller trapping force compared to the 2.07 µm sample. Further discussion will be conducted below.

2. *Threshold Current of LASER*

To generate the density inversion in LASER, enough amount of current must be supplied to pump electrons up to a higher energy state. In the handbook of the LASER, the threshold current was 35 mA, which is larger than the obtained value in TABLE III. Notably, the 3.0 µm sample showed meaningfully low threshold current, while the error range of the other samples all overlap. This anomaly may be substantiated by the friction particularly exerted on the 3.0 µm sample. The 3.0 µm sample has a large diameter and it was observed to be stuck or cling to the slide glass or cover glass. Therefore, the assumption that the drag force by water and the trapping force is in equilibrium does not fit well for the 3.0 µm sample. The additional friction exerted by slide glass or cover glass must be considered. It explains the deviation of the threshold current and low R^2 of the linear trend line for the 3.0 µm sample. The friction affects not only the threshold current but also the trapping force. The trapping force may be underestimated since the friction was not included in the force equilibrium.

C. Configuration of Beads in Multiple Trapping

The configurations of multiple beads are shown in FIG. 4a to FIG. 4c. The threshold velocity was briefly measured for the multiple beads trapping. Compared to that of a single bead trapping, the threshold velocity was decreased, which implies the decline of trapping force on one bead. However, the dwindled trapping force was not

exactly half, one-third, and one-fourth for two, three, and four beads trapping, respectively. The amount of decreased trapping force needs to be analyzed quantitatively. Also, the proposed configurations must be proved to be stable theoretically. By theoretical consideration, the new configurations might be found to be stable.

D. Additional Discussions

1. Deviation from the Ray-Optics Regime

The force exerted by light can be written as (1). Given that the intensity of the LASER in this experiment was 40 mW, the scale of force exerted by the LASER is about 10^{-10} N. The density of silica bead is $2648\,\mathrm{kg\,m^{-3}}$ [3]. If the light force and the gravity are in equilibrium for a spherical silica bead with zero porosity, the threshold radius R can be calculated as (13).

$$\frac{4}{3}\pi R^3 \rho g = \frac{nP}{c}, R = (\frac{3nP}{4\pi\rho c})^{1/3} \tag{13}$$

Thus, the scale of the radius is 10 µm scale. Since the wavelength of the LASER is 0.658 µm, which is comparable to the calculated radius, the ray-optics regime does not fit well for this experiment. Therefore, the quantitative analysis based on the ray-optics regime is impossible.

2. Additional Topics to Consider

Spherical beads were used in this experiment, however, there are many cases in which the sample to trap is not spherical. For a non-spherical sample, there are some stable equilibrium points where the LASER can stably trap it. For instance, considering a cubical bead with the ray-optics regime, the stable orientation is the direction that its diagonal line and the LASER beam is parallel. By the Brownian motion of the fluid containing the sample, it will change its orientation randomly. Therefore, the sample will be trapped by the LASER when it approaches the stable equilibrium orientation. To elaborate on the discussion, the quantitative theory for the non-spherical sample must be constructed, including not only the ray-optics regime but also other conditions.

In this experiment, the mode of LASER was TEM_{00}, of which the intensity profile is Gaussian. If the other mode was used, there could be multiple equilibrium points with different positions and intensities. Note that the stability of each equilibrium point may be different. The empirical approach to understanding the behavior of the optical tweezers with non-Gaussian intensity profiles needs to be tried. In addition, to generate the optical trap, it is enough to make a Gaussian intensity profile without coherence and monochromatic rays. However, the LASER possesses the advantage of focusing high-intensity light on a specific point.

V. CONCLUSION

To measure the trapping force of the optical tweezers, the viscosity of water was measured by the Brownian motion of beads. The randomness of the Brownian motion was proved by a linear Q-Q plot with a little deviation due to the net flow of water, which is challenging to consider accurately. With the assumption that the trapping force and the drag force are in equilibrium, the trapping force was obtained from the Stokes' drag force. It was claimed that Stokes' drag force might fail to give the exact drag force due to non-ideal factors such as turbulence or interactions between beads. The trapping force increased linearly as the current of the LASER increased, and then the threshold current was obtained from the x-intercept of the threshold velocity-current graph. The trapping force was maximal for the 2.07 µm sample because its size is similar to the LASER beam diameter. The deviation of the 3.0 µm sample was analyzed as an effect of friction between beads and the slide/cover glass. In addition, some stable configurations for multiple bead trapping were also found.

ACKNOWLEDGMENTS

I appreciate performing this harsh experiment with my dear coworkers, Seunghyun Moon and Gyujin Kim.

[1] P. Polimeno, A. Magazzu, M. A. Iati, F. Patti, R. Saija, C. D. E. Boschi, M. G. Donato, P. G. Gucciardi, P. H. Jones, G. Volpe, *et al.*, Optical tweezers and their applications, Journal of Quantitative Spectroscopy and Radiative Transfer **218**, 131 (2018).

[2] A. Ashkin, Forces of a single-beam gradient laser trap on a dielectric sphere in the ray optics regime, Biophysical journal **61**, 569 (1992).

[3] D. R. Lide, *CRC handbook of chemistry and physics*, Vol. 85 (CRC press, 2004).